IOP PUBLISHING JOURNAL OF PHYSICS D: APPLIED PHYSICS

J. Phys. D: Appl. Phys. **41** (2008) 234005 (11pp) doi:10.1088/0022-3727/41/23/234005

Positive and negative streamers in ambient air: modelling evolution and velocities

Alejandro Luque[1], **Valeria Ratushnaya**[1] **and Ute Ebert**[1,2]

[1] CWI, PO Box 94079, 1090 GB Amsterdam, The Netherlands
[2] Department of Physics, Eindhoven University of Technology, The Netherlands

Received 22 April 2008, in final form 11 June 2008
Published 20 November 2008
Online at stacks.iop.org/JPhysD/41/234005

Abstract

We simulate short positive and negative streamers in air at standard temperature and pressure. First, double-headed streamers in homogeneous electric fields of 50 kV cm^{-1} are briefly studied, and then we analyse streamers that emerge from needle electrodes with voltages of 10–20 kV in more detail. The streamer velocity at a given streamer length depends only weakly on the initial ionization seed, except in the case of negative streamers in homogeneous fields. We characterize the streamer evolution by length, velocity, head radius, head charge and maximal field enhancement. We show that the velocity of positive streamers is determined mainly by their radius and in quantitative agreement with recent experimental results both for radius and velocity. The velocity of negative streamers is dominated by electron drift in the enhanced field; in the low local fields of the present simulations, it is little influenced by photo-ionization. Initially it is puzzling that negative streamers can be slower than positive ones under similar conditions, both in experiment and in simulation, as negative streamer fronts always move at least with the electron drift velocity in the local field. We argue that this drift motion broadens the streamer head, decreases the field enhancement and ultimately leads to slower propagation or even extinction of the negative streamer.

(Some figures in this article are in colour only in the electronic version)

1. Introduction

Atmospheric pressure corona discharges are widely used in technology. Streamers, which are the basic building blocks of these discharges, focus a large part of the energy of the reactor into a small volume. As positive streamers emerge from pointed electrodes at lower voltages than negative ones [1, 2], recent investigations have largely focused on positive streamers. However, negative streamers are clearly present in many natural phenomena of atmospheric electricity such as lightning and sprite discharges [1, 3–5]. They are also of theoretical interest because they can be described by moving boundary models [6] and in some contexts can be related to the classical problem of viscous fingering in fluid dynamics [7]. Furthermore, modern high voltage supplies easily create negative streamers [2, 8, 9], and they are very promising for disinfection applications [10, 11] if electrical matching problems can be overcome. An experimental study of positive and negative streamers in air at standard temperature and pressure in a wide voltage range is available in [2].

The simulation of positive streamers in three spatial dimensions with cylindrical symmetry, meanwhile, is based on a large body of research. Pioneering work was done by Wang and Kunhardt [12] and by Dhali and Williams [13]. The use of more complete and realistic plasma-chemical models [14], better modelling of the electrode geometry [15, 16] and an efficient calculation of the non-local photo-ionization source [17, 18] have finally allowed simulation and experimental results to converge within a narrow range. Pancheshnyi *et al* [19] were able to predict the mean streamer velocity at varying pressures within a range of around 25% and thus question the role of photo-ionization versus fast electron detachment in repetitive positive streamer discharges in air [20]. Also remarkable was the reproduction of experimental results [21] of streamers in long gaps of 13 cm performed in [22].

Table 1. List of reactions with reaction rates in the model; they are taken from [19]. The effective temperature of electrons T_e as a function of the local electric field is taken from electron swarm experiments described in [29].

$N_2^+ + N_2 + M \rightarrow N_4^+ + M$	$k_1 = 5 \times 10^{-29}\,\mathrm{cm^6\,s^{-1}}$
$N_4^+ + O_2 \rightarrow O_2^+ + N_2 + N_2$	$k_2 = 2.5 \times 10^{-10}\,\mathrm{cm^3\,s^{-1}}$
$N_2^+ + O_2 \rightarrow O_2^+ + N_2$	$k_3 = 6 \times 10^{-11}\,\mathrm{cm^3\,s^{-1}}$
$O_2^+ + N_2 + N_2 \rightarrow O_2^+N_2 + N_2$	$k_4 = 9 \times 10^{-31}\,\mathrm{cm^6\,s^{-1}}$
$O_2^+N_2 + N_2 \rightarrow O_2^+ + N_2 + N_2$	$k_5 = 4.3 \times 10^{-11}\,\mathrm{cm^3\,s^{-1}}$
$O_2^+N_2 + O_2 \rightarrow O_4^+ + N_2$	$k_6 = 1 \times 10^{-09}\,\mathrm{cm^3\,s^{-1}}$
$O_2^+ + O_2 + M \rightarrow O_4^+ + M$	$k_7 = 2.4 \times 10^{-30}\,\mathrm{cm^6\,s^{-1}}$
$e + O_4^+ \rightarrow O_2 + O_2$	$k_8 = 7.3 \times 10^{-08}(1/T_e)^{1/2}\,\mathrm{cm^3\,s^{-1}\,K^{1/2}}$
$e + O_2^+ \rightarrow O + O$	$k_9 = 1.8 \times 10^{-12}(1/T_e)\,\mathrm{cm^3\,s^{-1}\,K}$
$e + O_2 + O_2 \rightarrow O_2^- + O_2$	$k_{10} = 5.4 \times 10^{-32}(1/T_e)\,\mathrm{cm^6\,s^{-1}\,K}$
$O_2^- + O_4^+ \rightarrow O_2 + O_2 + O_2$	$k_{11} = 1 \times 10^{-07}\,\mathrm{cm^3\,s^{-1}}$
$O_2^- + O_4^+ + M \rightarrow O_2 + O_2 + O_2 + M$	$k_{12} = 2 \times 10^{-25}\,\mathrm{cm^6\,s^{-1}}$
$O_2^- + O_2^+ + M \rightarrow O_2 + O_2 + M$	$k_{13} = 2 \times 10^{-25}\,\mathrm{cm^6\,s^{-1}}$

In early work, the non-local ionization mechanism through photons was replaced by background ionization, and positive and negative streamers looked fairly similar. An example of a simulation of a double-headed streamer that is completely dominated by the assumption of the initial ionization distribution can be found in [23]. Since photo-ionization was introduced as a non-local ionization mechanism in air to explain the propagation of positive streamers, work mainly concentrated on positive streamers, and only a few groups of authors have investigated negative streamers in air with photo-ionization. Babaeva and Naidis have compared positive and negative streamers emerging from pointed electrodes in a short paper in 1997 [24], Liu and Pasko have investigated doubled-headed streamers in homogeneous fields [25, 26] and the present authors have studied the influence of photo-ionization on propagation [18] and interaction [27] of streamers of both polarities.

This paper is devoted to a systematic study, characterization and comparison of positive and negative streamers in ambient air. It is organized as follows. In section 2 we describe our model and the initial conditions. Section 3 treats double-headed streamers in homogeneous fields, their dependence on the ionization seed chosen as a starting point for the simulations and their basic mode of propagation. Section 4 treats positive and negative streamers emerging from needle electrodes; streamers of both polarities are characterized by velocity, field enhancement, head radius and head charge; characteristic differences are found. Their velocities are dominated either by the head radius for positive streamers or by the enhanced field for negative streamers. Section 5 shows a convincing comparison with the experiments in [2]. Finally, we summarize our main results in section 6. Appendix A contains the charge simulation technique (CST) for the needle electrode.

2. Model

2.1. Model formulation

We use a fluid model of air that contains electrons and six species of ions: N_2^+, O_2^+, N_4^+, O_4^+, $O_2^+N_2$ and O_2^-. While electrons diffuse and drift in a self-consistent electric field, the ions due to their much larger mass can be approximated as immobile. We consider 15 reactions among the species, taken from [19] and listed in table 1, plus photo-ionization. The model equations are

$$\frac{\partial n_e}{\partial t} = \nabla \cdot (n_e \mu_e \boldsymbol{E}) + D_e \nabla^2 n_e + S_i + S_{ph} + K_e, \tag{1}$$

$$\frac{\partial [N_2^+]}{\partial t} = \frac{[N_2]}{[N_2] + [O_2]} S_i + K_{N_2^+}, \tag{2}$$

$$\frac{\partial [O_2^+]}{\partial t} = \frac{[O_2]}{[N_2] + [O_2]} S_i + S_{ph} + K_{O_2^+}, \tag{3}$$

$$\frac{\partial [Z_i]}{\partial t} = K_{Z_i}, \tag{4}$$

where $\boldsymbol{E}$ is the local electric field, n_e is the electron density, μ_e is the electron mobility, D_e is the electron diffusion coefficient and $[Z]$ is the density of species Z. The densities of N_2 and O_2 are taken as 80% and 20%, respectively, of the total gas density. The reactions of table 1 are taken into account by the source terms K_Z. For example, electron attachment decreases the electron density at a rate

$$K_{e,\mathrm{attachment}} = \left.\frac{\partial n_e}{\partial t}\right|_{\mathrm{attachment}} = -\left.\frac{\partial [O_2^-]}{\partial t}\right|_{\mathrm{attachment}} = -k_{10} n_e [O_2]^2. \tag{5}$$

The change in the neutral densities $[N_2]$, $[O_2]$ in streamers is neglected. The impact ionization S_i is given by Townsend's approximation,

$$S_i = n_e \mu_e |\boldsymbol{E}| \alpha(|\boldsymbol{E}|) = n_e \mu_e |\boldsymbol{E}| \alpha_0 e^{-E_0/|\boldsymbol{E}|}, \tag{6}$$

where α_0 is the ionization cross section and E_0 is the threshold field. The non-local photo-ionization is

$$S_{ph}(\boldsymbol{r}) = \frac{\xi}{4\pi} \frac{p_q}{p + p_q} \cdot \int \frac{h(p|\boldsymbol{r} - \boldsymbol{r}'|) S_i(\boldsymbol{r}') \mathrm{d}^3(p\boldsymbol{r}')}{|p\boldsymbol{r} - p\boldsymbol{r}'|^2}, \tag{7}$$

where ξ is a proportionality constant, p is the gas pressure, $p_q = 60\,\mathrm{Torr} = 80\,\mathrm{mbar}$ and h is the absorption function of photo-ionizing radiation. The integral in (7) is approximated by two Helmholtz differential equations as described in [18] which is computationally much more efficient than solving the integral.

Finally, the electric field is calculated self-consistently from the Poisson equation:

$$\epsilon_0 \nabla \cdot \boldsymbol{E} = eq, \tag{8}$$

where q is the net spatial charge.

All our simulations are performed at standard pressure and temperature. We assume cylindrical symmetry of the streamer and we solve the model numerically by means of adaptively refined grids [28]. The finest grid cells are $\Delta r = \Delta z = 2.3\,\mu$m which is the minimal ionization length $1/\alpha_0$.

We performed numerical experiments in two geometries: the simplest one is defined by plane parallel electrodes with fixed electrical potential, therefore we impose Dirichlet boundary conditions to the potential. A more complex geometry is given by a needle electrode, which we simulate by means of a simplified version of the CST, as detailed in appendix A.

2.2. Initial electron distribution and background ionization

In all our simulations the initial ionization is confined to a localized Gaussian seed while the rest of the simulation domain does not contain any free charges. Namely, we model the initial electron and N_2^+ densities as

$$n_e = [N_2^+] = A e^{-\frac{(\boldsymbol{r}-\boldsymbol{r}_0)^2}{\sigma^2}}, \tag{9}$$

where $\boldsymbol{r}_0$ is the location of the centre of the seed, σ is the density e-folding radius and A is the peak density, related to the total number of initial electrons and ions N by $A = N/\pi^{3/2}\sigma^3$.

We remark that the formation of the initial seed is never included in current fluid simulations; this earlier stage of evolution is a matter of current research; see, for example, [30, 31]. In general, low initial electron densities or the proximity to an electrode can require a description on particle level [29, 31, 32]. This is also true for the natural background ionization due to radioactivity and cosmic radiation that is commonly assumed to be 10^3–10^4 free electrons per cm^3 (see [20] for a detailed discussion). Within volumes of $(100\,\mu\text{m})^3$ that characterize the structures within the streamer head (see figures 1 and 4), this corresponds to 10^{-3}–10^{-2} free electrons in the relevant volume. These numbers represent probabilities rather than densities. Within a density approximation, we therefore neglect them. We have tested in our simulations that an inclusion of such 'densities' does not change our results. This is consistent with analytical estimates of the growth or decay of electron densities in the corresponding field.

Our results in section 4 mimic experiments as reported in [2, 33], where the streamers propagate into virgin air in a needle-plane electrode geometry, and where the voltage rise-time is so short that it can be neglected. However, the pre-ionization background may be significantly higher for repetitively pulsed discharges [20] or for slow potential rise-times [34], causing their different appearance in such experiments.

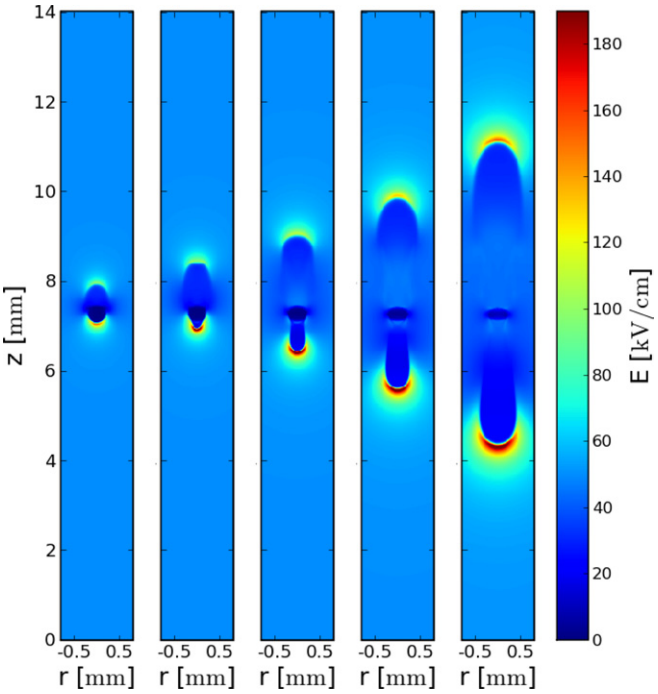

Figure 1. Electric field of a double-headed streamer extending between two planar electrodes, plotted at equal time steps of 1.2 ns. The negative front is propagating upwards, the positive front moves downwards. The number of particles N in the initial seed is 6×10^{10}, and the e-folding radius is $\sigma = 74\,\mu$m. Note that the lateral borders of the figure do not correspond to the full computational domain, $|r| < 4$ mm.

3. Double-headed streamers in homogeneous background fields

3.1. Motivation

We first study streamers in homogeneous background fields. Most streamer experiments are performed in needle-plane [2, 33, 34], wire-plane or wire-cylinder geometries [9], some also between planar electrodes with a protrusion [21, 35]; here the protrusion is used as the inception point of the discharge. Experiments of streamers between planar electrodes created with a laser were difficult to interpret [36]. The last two experiments were particularly designed to study streamers in homogeneous background fields while the inception from curved electrodes is much easier. But even if one electrode is a needle or a wire and the other one a plane, once the streamer tip approaches the planar electrode, the background field is again well approximated by a homogeneous field. Finally, the electric field responsible for sprite discharges, located between a charged thundercloud and the ionosphere, is rather homogeneous.

3.2. Simulations and dependence on the initial ionization seed

A streamer discharge in a homogeneous field is initiated by a localized ionization seed created, for example, by a cosmic particle shower or by an electric field inhomogeneity around a suspended particle. If the field is above $\sim$30 kV cm^{-1},

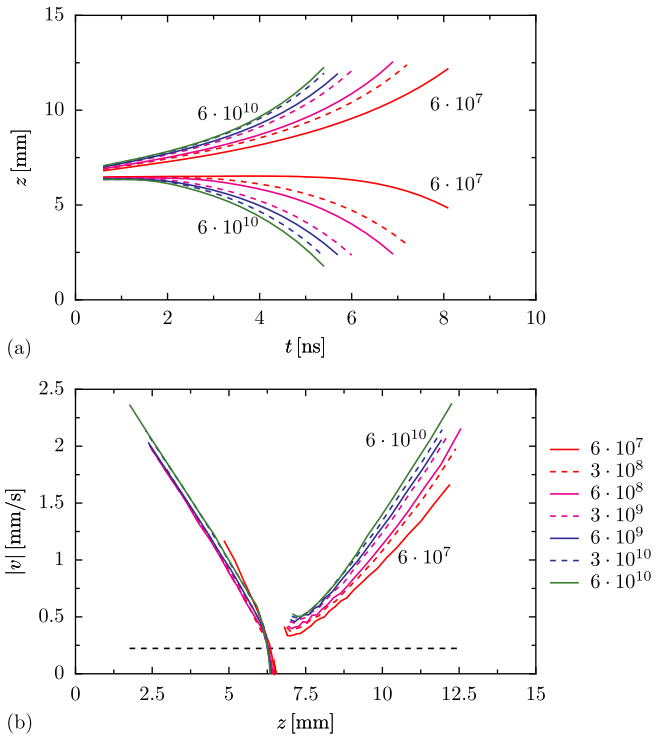

Figure 2. (*a*) Position $z(t)$ of the negative (upper) and positive (lower) fronts of a double-headed streamer as a function of time t. The streamer evolves between two planar electrodes with a background field $E_0 = 50\,\mathrm{kV\,cm^{-1}}$ as shown in figure 1. The distance between the electrodes is 14 mm. The different colours correspond to different numbers N of initial electrons and N_2^+ ions ranging from 6×10^7 to 6×10^{10} as indicated in the figure (the seed therefore is electrically neutral). (*b*) The same data, now plotted as the absolute values of velocities $v(z)$ of the negative (right) and positive (left) fronts as a function of the front location z. Note that each front propagates in a different direction, but the absolute value of the velocity is plotted to help the comparison. The dotted horizontal line indicates the velocity $v^*(E_0)$ of a planar negative ionization front in the background field E_0.

a small seed first can undergo an avalanche phase where the ionization level increases exponentially and then, once there are significant space-charge effects, it reaches the streamer regime [30, 31]. If the field is below threshold, a seed of finite size is required that after drift separation of charges immediately enters the streamer phase.

To investigate whether the initiation mechanism in a field above threshold has a lasting effect on the propagation of a streamer, we run several simulations with different initial seeds. The background field was $E_0 = 50\,\mathrm{kV\,cm^{-1}}$ and the seeds had a spherical Gaussian profile with an e-folding radius of 74 μm located at the centre of a 14 mm gap, creating a double-headed streamer. The lateral computational boundary was located at $r = 4\,\mathrm{mm}$. The temporal evolution of the streamer shape is illustrated in figure 1 for a particular seed. Figure 2(*a*) shows the position z of the two ionization fronts as a function of time t; it shows that both fronts accelerate in time, and that the fronts with the particle rich seeds are ahead in evolution to those that start with a weaker seed; they propagate faster at any particular time both on the positive and on the negative side.

The front velocity v as a function of time t is simply the derivative of the curves in figure 2(*a*), and $v(t)$ strongly depends on the size of the initial seed both for the positive and for the negative front. On the other hand, figure 2(*b*) shows the absolute value of the velocity v as a function of front location z—this is the observable typically measured in the experiments. Here the curves $v(z)$ for the positive fronts essentially overlap for different seeds while those for the negative fronts do not: the negative streamers with the largest seed have the largest velocities $v(z)$ after they have propagated the same distance.

3.3. Discussion of inception and propagation of positive and negative streamers

We now discuss the physical mechanisms causing the different dependences of $v(z)$ on the initial seed. The horizontal dotted line in figure 2(*b*) indicates the velocity $v^*(E_0)$ where

$$v^*(E) = |E| + 2\sqrt{D|E|\alpha(|E|)} \tag{10}$$

is the velocity of a planar negative ionization front in a field E in the absence of photo-ionization in dimensionless units [37, 38]; it is given by the local electron drift velocity $|E|$ augmented by the combined effect of electron diffusion D and impact ion ionization $\alpha(|E|)$. The velocity $v^*(E_0)$ evaluated in the background field E_0 is a lower bound for the velocity of a negative ionization front with field enhancement and with photo-ionization as can indeed be seen in the figure. Obviously, the negative front will always propagate at least with the electron drift velocity in the local electric field. If the initial seed is stronger, field enhancement will build up faster while the front is already in motion, and at each position z, the front is faster than for a weaker seed. The positive front, on the other hand, has no lower bound for its velocity. The positive discharge side stays at rest until photo-ionization has built up a sufficient electron concentration for the streamer to start. This means that the inception time now strongly depends on the seed, but once the positive streamer propagates, it does it with a similar velocity v as a function of the position, rather independently of the seed.

In view of the experimental results, a most interesting question is the comparison of the velocities of positive and negative streamers. If we fix the time elapsed after the seed of the double-headed streamer is created, the negative streamer is faster than the positive one. If, on the other hand, one compares the velocities at a fixed distance from the initial seed, the picture is different: for small distances, the negative streamers are faster, but they are overcome by the positive ones at larger distances from the initial seed. Note also that the differences between positive and negative streamers become smaller the larger the initial number of particles.

The only other studies of double-headed streamers with photo-ionization in a homogeneous electric field are performed by Liu and Pasko [25, 26]; in particular, table 2 in [25] shows that the characteristics of streamer propagation, namely field enhancement in the streamer head and field screening in the streamer interior are stronger on the positive streamer head, and that the positive streamer is faster. This is found in air models applicable to a height of 0, 30 and 70 km in the atmosphere.

3.4. Why positive streamers can be faster than negative ones

The larger velocity of the positive streamers is surprising if one takes into account that for identical field enhancement and identical electron distribution in the leading edge of the ionization front, the negative front will always be faster [37] as electron drift supports propagation of negative fronts and acts against it for positive fronts. However, inspection of figure 1 shows that the positive streamer is more focused and the field at its head is more enhanced. Ultimately, electron drift leads to a 'dilution' of head focusing and field enhancement in negative streamers and makes them run slower at a given distance from the ionization seed.

4. Streamers in needle-plane geometries

The study of streamers disconnected from electrodes in homogeneous fields already gives a good qualitative insight into many of their properties. However, laboratory experiments and engineering applications are mostly done in inhomogeneous fields and streamers emerge from pointed electrodes. Then the background electric field before the initiation of the discharge is typically considerably larger than the threshold field of 30 kV cm^{-1} near the needle electrode and decays to lower values further away. We here study positive and negative streamers emerging from a needle electrode and propagating towards a planar electrode. This electrode configuration was implemented by means of the CST as described in appendix A.

4.1. Weak dependence on the initial conditions

In order to study how the streamer behaviour depends on parameters, we performed a number of different simulations. The first observation is that in contrast to the case of homogeneous fields, in inhomogeneous fields the initial seed affects the propagation of the streamer only slightly, even when considering the streamer velocity v as a function of time t. This is illustrated in figure 3 where the positions z of streamers as a function of time t are shown for several initial seeds—this plot corresponds to figure 2(a). The seeds are placed at the top of the gap and have spherical Gaussian profiles with radius 92 μm and between 6×10^6 and 3×10^9 particles. The positions of the positive streamers are independent of the initial seed up to 5%; for the negative ones, this is 6%. Also the front velocities are rather independent of the initial seed.

For positive streamers in needle-plane geometries, this effect was found before by Pancheshnyi *et al* [39]. The reason is probably that in the high-field region near the needle electrode, the seed grows very rapidly compared with the slower evolution in the lower fields away from the needle.

4.2. Positive streamers at different voltages: electrodynamic characterization

We now analyse positive streamers in the needle-plane geometry in more detail. We run simulations of positive streamers in a short gap of 7 mm gap at a voltage of 10.5, 14 and 21 kV. The needle electrode had a radius $R_{\text{needle}} = 0.2$ mm and a length $L_{\text{needle}} = 2$ mm. An example of the evolution of the streamers is shown in figure 4(a).

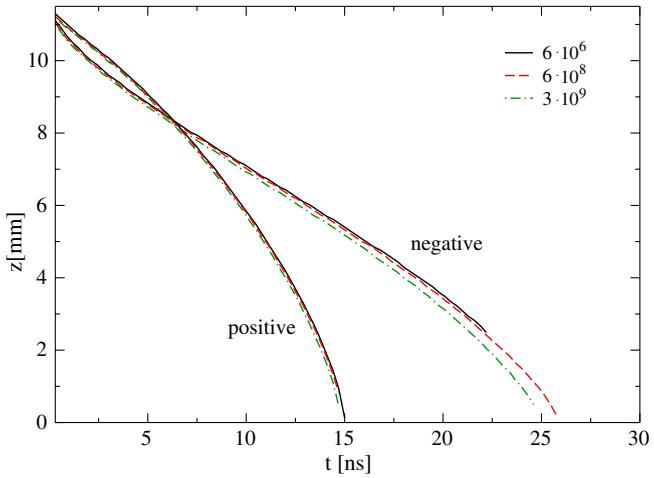

Figure 3. Front propagation of negative and positive streamers for different seeds between needle-plane electrodes. The gap is $L = 11.5$ mm long with an applied voltage of 23 kV; the needle parameters are $L_{\text{needle}} = 2.3$ mm, $R_{\text{needle}} = 0.26$ mm. Different line styles correspond to different number of particles in the initial seed.

Many experiments show branched trees of many streamers [21, 33] while most simulations [19, 40] up to now treat only one in cylindrical symmetry, as fully 3D simulations [27] only now come within reach. But we expect a propagating streamer head at some distance from the electrode to be characterizable by a few electrodynamic properties, independently of the number of streamers in the system. Such concepts were previously suggested in Russian literature [3, 41–43], but charge conservation was not properly incorporated, as discussed in [44]. To develop a better understanding of the electrodynamics of the streamer heads, we characterize them at each time by the streamer channel length L, velocity v, maximal field enhancement E_{max}, radius R and charge in the streamer head Q.

These quantities are defined and measured as follows. The streamer tip is the point on the propagation axis where the absolute value of the charge density is maximal. The space-charge layer of the streamer is then defined as the volume around the streamer tip where the absolute value of the charge density is larger than half of its maximum value. The streamer length L is the separation between the needle electrode and the streamer tip. The streamer velocity is simply $v = \mathrm{d}L/\mathrm{d}t$. The enhanced field E_{max} is defined as the maximum of the electric field strength.

The definition of a streamer radius is somewhat more involved. We are mainly interested in characterizing the shape of the space-charge layer. Hence we followed this procedure: for each z we took the radius r with the highest charge density. This gives us a $r(z)$ curve that we restrict to the points inside the space-charge layer. This curve is fitted to a circle and we take the resulting radius as the radius of the streamer, R.

The head of the streamer is precisely defined as the region of the propagating streamer head with length R. The charge in the head Q is defined as the net charge content inside that region.

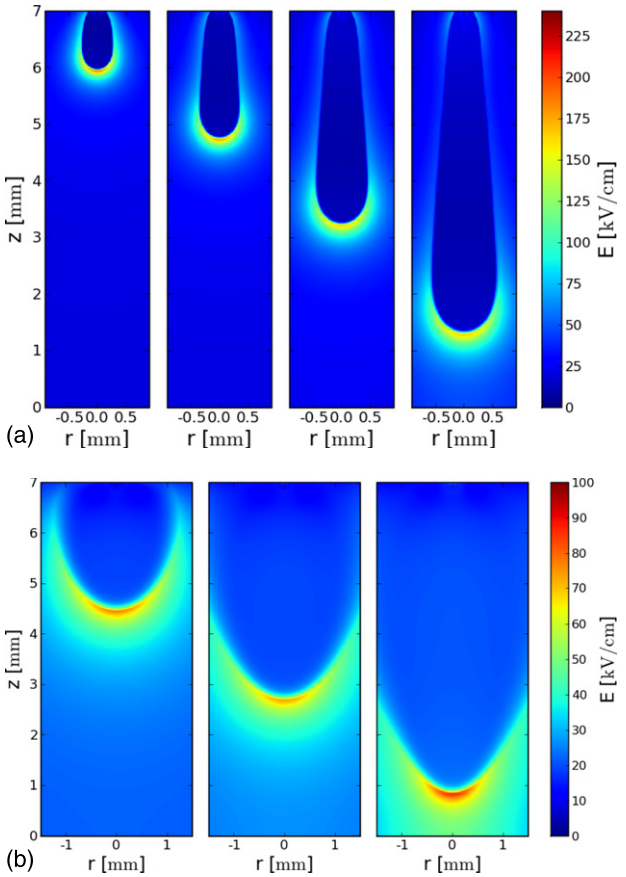

Figure 4. Electric field created by a propagating streamer in a needle-plane geometry plotted at equal time steps. Note that the computational domain extends beyond the lateral borders of the plot. (*a*) A positive streamer at time steps of 2.7 ns in a voltage of 14 kV, (*b*) a negative streamer at time steps of 4.5 ns also in a voltage of 14 kV.

In figure 5, the evolution of three simulations with different voltages is shown. The array shows each observable as a function of each other, hence searching for consistent relationships between the streamer characteristics.

For example, in figure 5 one can observe that for each run the charge content inside the streamer depends roughly linearly on the streamer length, but this dependence is not consistent among different voltages. The relationship between charge content and enhanced field, on the other hand, looks more consistent, although non-linear. Note also that one should differentiate between the three phases of evolution shown in figure 5: (1) a short inception phase close to the point electrode, (2) streamer propagation, which takes most of the time and (3) interaction with the planar electrode, shortly before the end. In our discussion we will focus only on the phase of streamer propagation.

The overall evolution shown in figure 5 can be summarized as follows: as the streamer advances, it becomes thicker and faster and the total charge in the streamer head increases while the enhanced electric field decreases.

4.3. The velocity of positive streamers

While for a negative streamer, the velocity v cannot become smaller than the electron drift velocity $|E_{\max}|$ in the locally enhanced field, for the positive streamer the velocity v increases while the field enhancement $|E_{\max}|$ decreases. In the experimental investigation [2], the completely empirical relation

$$v \approx \frac{0.5d^2}{\text{mm ns}} \tag{11}$$

between velocity v and diameter d of positive streamers in air at standard temperature and pressure was fitted to the experimental data (in figure 6(*b*) of [2]). In figure 5, the plots of v as a function of radius R also lie more or less on one line. In figure 6 we therefore compare the $v(R)$ plot of our simulation results with the experimental data [2] and the empirical fit (11) to these experiments. One can see that the experimental data and the results of our simulations are in good agreement. When interpreting the figure, it should be noted that the simulations measure the *geometrical* radius of the space-charge layer, also called 'electro-dynamic radius', while an experiment measures the visible, or radiative, radius. There can be a significant difference between both measures; in [19] it is estimated that the electrodynamic radius is about twice the radiative radius.

A positive streamer propagates due to the photo-ionization in front of its head. Comparing the head radius with the photo-ionization lengths [27], the hypothesis of Kulikovskii [40] that the streamer radius would be determined by the photo-ionization length can be clearly discarded. The photo-ionization absorption is fitted by two lengths scales, one of them essentially negligibly small and the other much larger than the head radius [18, 27]. Free electrons created by photo-ionization are therefore available throughout the region where the electric field is above the ionization threshold. Therefore the streamer velocity will be determined mainly by the size of the region where further electron multiplication by impact is efficient. This region, in turn, is roughly determined by two factors: the enhanced electric field and the electrodynamic radius of the streamer. In figure 5 we see that the radius varies much more than the enhanced field, which explains the qualitative relation between velocity and radius.

4.4. Negative streamers at different voltages: electrodynamic characterization

We investigated negative streamers also in a 7 mm gap with applied voltages of 10.5 and 14 kV. The electrode geometry was the same as for positive streamers. The evolution of the spatial structure is illustrated in figure 4(*b*). As in the case of the homogeneous field in figure 1, the negative streamer is broader and the field is less enhanced.

Figure 7 shows the relationship between relevant (electro-) dynamic quantities during the evolution of these two streamer simulations. See above for a discussion and interpretation about this representation of the streamer evolution. Note that also for negative streamers we focus on the propagation far from the electrodes.

The streamer in the lower voltage (circles) becomes slower, the enhanced field eventually drops below the threshold for impact ionization, the head charge disappears and the radius diverges. At that instant of time, the remaining electrons from the streamer head continue to drift towards the planar electrode,

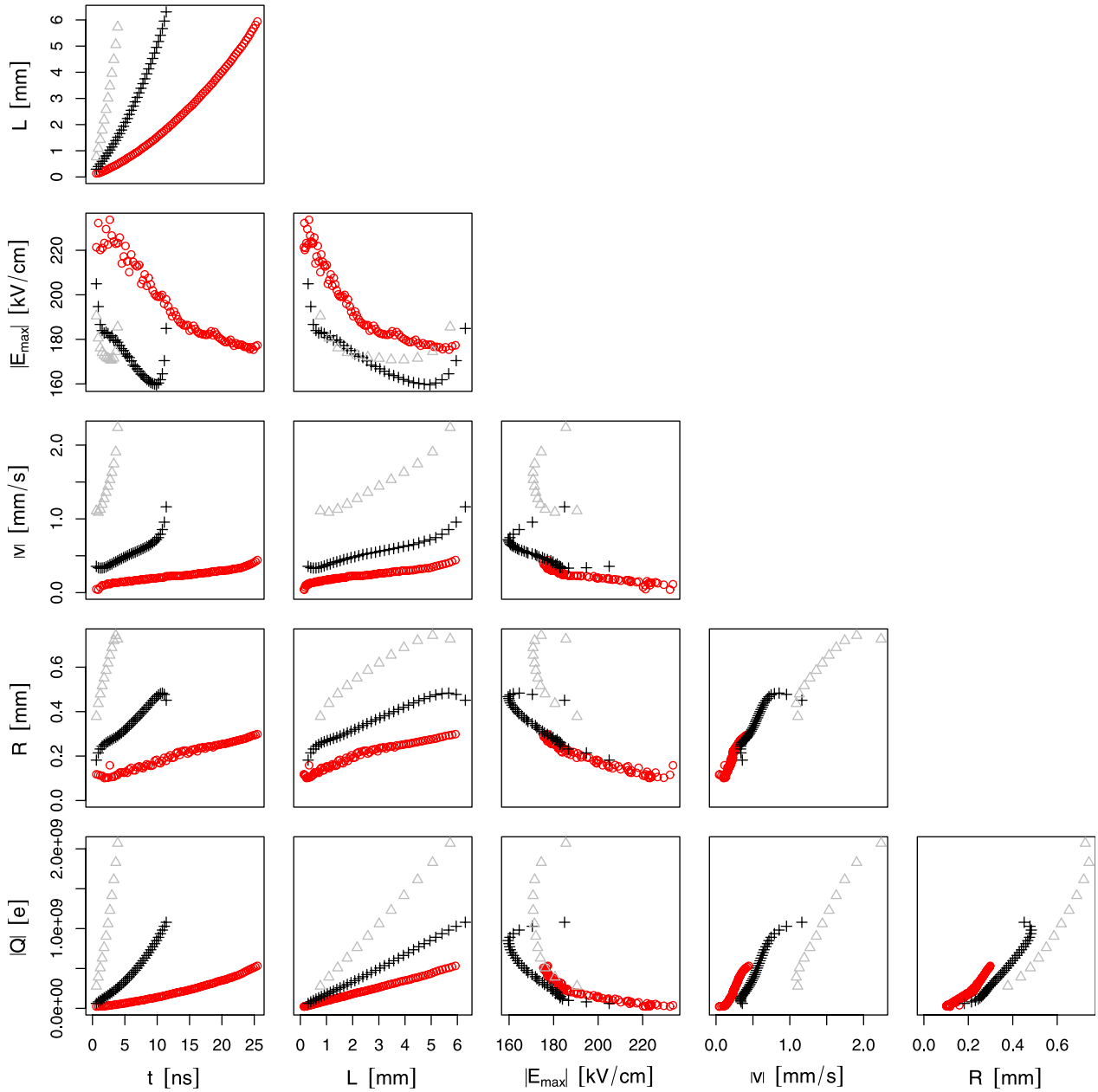

Figure 5. Characterization of positive streamers by their main (electro-)dynamical variables, namely time t, length L, maximal field E_{max}, velocity v, head radius R and charge in the streamer head Q. The picture shows each variable as a function of each other variable. The array of pictures makes the possible correlations between pairs of observables visible. Circles correspond to a voltage of 10.5 kV, crosses to 14 kV and triangles to 21 kV. Note that all plots are qualitatively similar for different applied voltages. Remarkably, the plots of streamer velocity v as a function of radius R nearly fall on the same line for different voltages.

but the impact ionization ceases to be efficient and the streamer mode of propagation stops. This is probably the generic way how a negative streamer extinguishes, quite different from the one reported for positive streamers in [45]. The streamer in the higher voltage undergoes a similar intermediate evolution. However, eventually the proximity of the planar electrode again enhances the field and the streamer reaches the electrode.

4.5. Velocity of negative streamers

As already discussed above and in sections 3.3 and 3.4, negative streamers propagate not only due to photo-ionization but also due to electron drift. For the velocity, this implies a stronger dependence on the enhanced field, which thus overcomes the dependence on the radius. In fact, comparison of figures 5 and 7 shows that the velocity of positive streamers increases with radius while the field enhancement decreases; the velocity of negative streamers, on the other hand, increases with field enhancement while the radius decreases. Indeed, figure 7 shows a very clear correlation between velocity v and field enhancement E_{max} for negative streamers that we now analyse further.

Actually, one can compare the actual velocities with the velocity $v^*(E_{max})$ where $v^*(E)$ is given in equation (10). The velocity $v^*(E_{max})$ is the velocity of a planar fully relaxed

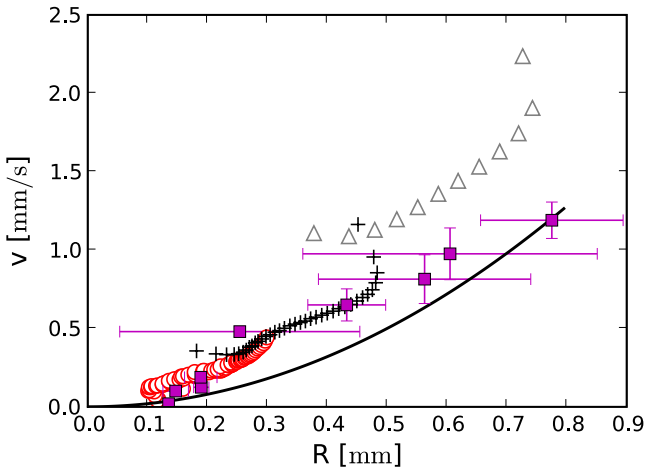

Figure 6. Relationship between velocity v and radius R of positive streamers. The symbols ○, + and △are simulation results as presented in figure 5, symbol □ and the continuous line represent, respectively, the measurements and empirical fit (11) of [2].

negative streamer front in a field E_{max} when the effect of photo-ionization is neglected. Figure 8 shows the simulation data for $v(E_{max})$ from figure 7 and the function $v^*(E_{max})$ for comparison. The coincidence is strong. Deviations mainly come from the fact that the analytical equation is a lower bound to the actual velocity as photo-ionization is neglected (for a comparison of simulation data without photo-ionization with the analytical formula we refer to [6, 7]).

One should remark here that the background electric field under which the streamer propagates most of the time is quite low and hence one does not observe a buildup of the ionization level in front of the streamer as in the high-field case of [18]. Therefore, we do not observe a transition to a regime dominated by photo-ionization.

4.6. Comparison of positive and negative streamer simulations

We here directly compare the propagation of a positive and a negative streamer in a longer gap of 11.5 mm than considered above in needle-plane geometry. For both positive and negative streamers the applied voltage is $V = 23$ kV. The radius of the needle is $R_{needle} = 0.26$ mm and its length is $L_{needle} = 2.3$ mm. The position as a function of time was already presented in figure 3 where it was shown that the evolution depends only very weakly on the initial ionization seed. The figure shows that the negative streamer initially is faster, but it is soon overtaken by the positive one.

In figure 9 we show the spatial profiles of the electric field on the streamer axis for a number of time steps; the streamers are propagating to the left. The electric field at the positive streamer heads is much more enhanced than on the negative ones. This larger field enhancement is due to the smaller radii of the positive streamers that consecutively propagate much faster. Also the field inside the streamer channel is screened less for negative streamers. We note that in the only other comparable simulation of positive and negative streamers by Babaeva and Naidis [24], the field inside the negative streamer channel is higher as well, but figure 6 of that paper shows that their negative streamers are faster than their positive ones, though there is also a consistency problem between their figures 6 and 7 and positive and negative streamer velocities are not compared in the text.

5. Comparison with experiments

Experiments [2, 9] show that positive and negative streamers in ambient air driven by voltages above 60 kV have qualitatively similar behaviour. On the other hand, there are major differences below 40 kV [2]. Positive streamers form at lower applied voltages, they are faster, longer and thinner. Our simulations at voltages between 10.5 and 21 kV in shorter gaps reproduce all these features.

5.1. Inception

While the full inception process in interaction with the electrode needle surface is not part of the present simulations, we observe that positive streamer inception is not very sensitive to the initial ionization seed while the negative streamer formation depends on it, at least in homogeneous fields.

5.2. Velocity

Close to the needle electrode, the electrons of the negative ionization seed drift outwards in the local field and are faster. However, just the lack of outward drift motion in the positive seed leads eventually to a larger field enhancement and ultimately to a faster propagation of the positive streamer at the same distance from the electrode.

Experimental measurements of the velocity of positive streamers are very well fitted by the empirical equation (11) that relates their velocity to their radius. Figure 6 shows that this equation also fits our simulation results quite well without any fit parameter.

5.3. Diameter

The negative streamers are thicker and less focused, both in simulations and in experiment. The minimal diameter of positive streamers in our simulations is about 0.2 mm, identical to the minimal diameter reported in experiments [2, 33, 34]. It should be noted, however, that the definition of the radius might differ between experiments and simulations as discussed in section 4.3.

5.4. Length and extinction

In a potential of 10.5 kV, the negative streamers extinguish after less than 2 mm, while the positive ones reach the planar electrode at 7 mm distance. In fact, in the experimental paper [2], discharges of 2 mm length are not called streamers, and the extinction of these very short negative discharges is in agreement with experiment. At 14 kV, our simulated negative streamers do reach the planar electrode, but they are helped by a strong initial ionization seed and a short gap. Simulations in longer gaps are in progress.

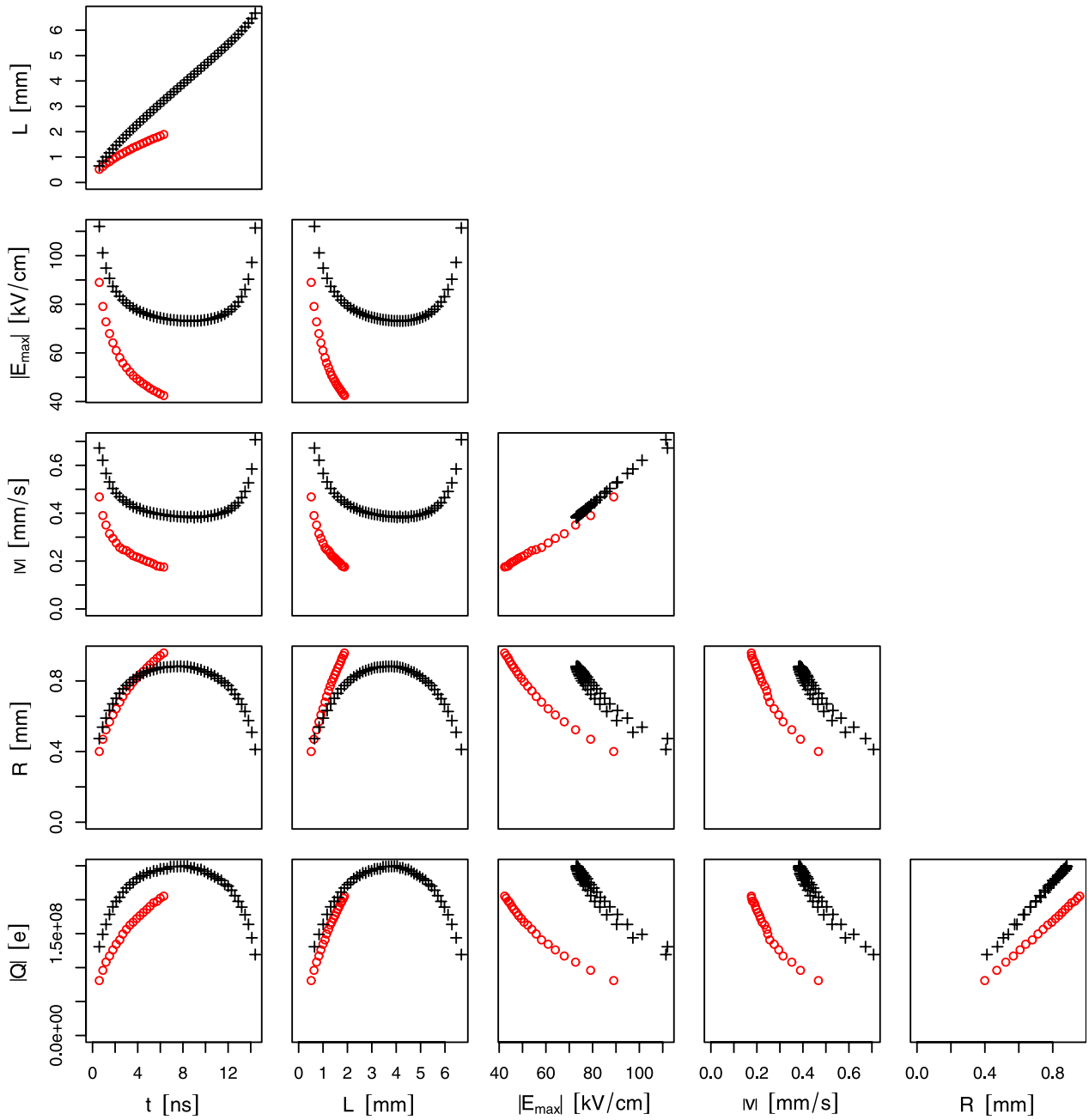

Figure 7. Characterization of negative streamers by their main (electro-)dynamical variables, the presentation is the same as in figure 5 for positive streamers. All simulations were performed in the same geometry as for the positive streamers, with applied voltages 10.5 kV (red circles) and 14 kV (black crosses). Note that in the low voltage case, the enhanced field ceases to be strong enough to sustain the streamer propagation.

6. Summary and outlook

We have studied the propagation of double-headed streamers in a homogeneous field and the inception and propagation of positive and negative streamers emerging from needle electrodes. We have shown that for spatially concentrated ionization seeds containing from about 10^7 to about 10^{10} electron–ion pairs, the streamer velocity at a given streamer length depends only weakly on the seed, except for the case of negative streamers in homogeneous fields. We have found qualitative and quantitative agreement with experiment as summarized in section 5.

We have shown that the relations between velocity v, radius R, field enhancement $E_{\max}$ and head charge Q that characterize the propagation of a streamer, differ qualitatively between streamers of different polarities. The velocity of a positive streamer in air is determined mainly by its radius, in accordance with the empirical fit formula (11), while that of a negative one is dominated by the enhanced electric field and well approximated by $v^*(E_{\max})$ where $v^*(E)$ is the velocity of a planar negative ionization front in the absence of photo-ionization. These statements on the simulations hold in the voltage range 10–20 kV in gaps of 7 or 11.5 mm length. Longer gaps and higher potentials will be investigated in the future.

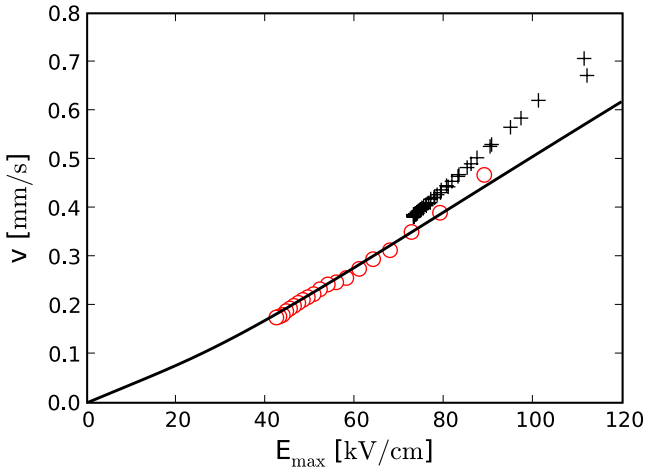

Figure 8. Relationship between velocity v and enhanced field $E_{\max}$ for negative streamers. The symbols are simulation results as presented in figure 7, the continuous line represents the velocity of a planar front without photo-ionization $v^*(E_{\max})$ (10).

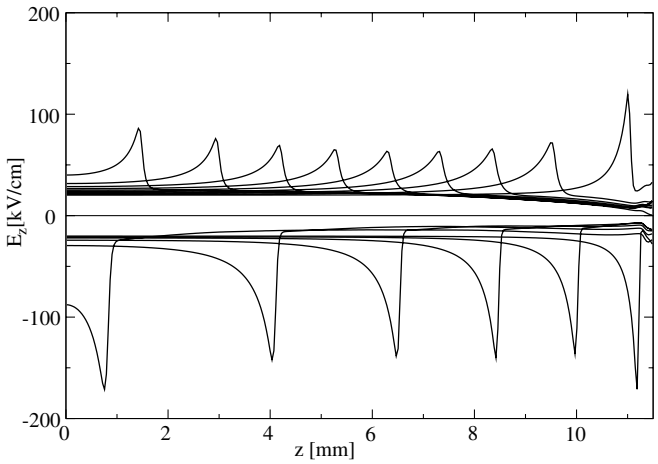

Figure 9. Electric field on the streamer axis at equal time steps of 3 ns for negative (upper) and positive (lower) streamers propagating to the left. The number of particles in the initial seed is 6×10^8.

The characterization of the streamer head by velocity, radius, field and charge is a first step towards an electrodynamical characterization of streamer head and channel. Such models were already sketched in [3, 41–43], however, they need to take care of the polarity dependence of streamers, and they have to be made consistent with charge conservation [44].

The fact that in experiments [2] positive streamers moved faster than negative ones initially was quite puzzling from a theoretical point of view. As electron drift acts against positive and in favour of negative streamers, a streamer with identically formed space-charge layer in its head will always move faster, if it is negative. However, the simulations show that the electron drift does not necessarily help the negative streamer to propagate; rather the outward drift motion that is essentially linear in the field, leads to a growth of the head radius and a subsequent 'dilution' of field enhancement. The growth of the positive streamer depends more non-linearly on the local field through impact ionization; therefore it stays thinner, the field is enhanced more and subsequently it propagates faster. In experiments, this asymmetry is found to decrease with increasing voltage; whether simulations show the same, will also have to be investigated in the future.

Streamer physics is an exciting and widely open field, and it is amazing to note how little their polarity dependence has been characterized up to now, both experimentally and theoretically. Of course, the study of single streamers is only one problem in a range of phenomena, other questions concern streamer branching [46, 47], interactions [7, 27], particle aspects [29, 31], the full inception process near an electrode or the electrodynamical characterization of multi-streamer processes.

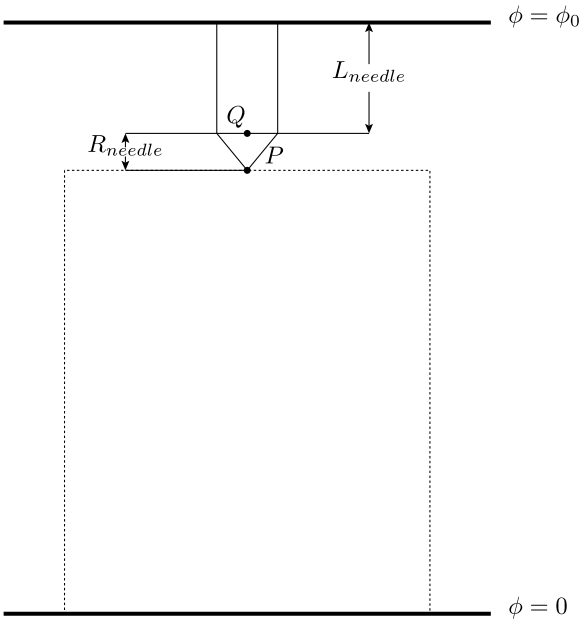

Figure A1. Implementation of a needle electrode using the CST with a single charge. The particles are restricted to the rectangular domain below the needle, while the electrostatic field is solved in a larger domain limited by the two planar electrodes.

Acknowledgments

AL is financially supported by STW under contract number 06501, and VR by IOP-EMVT under contract number 062126B.

Appendix A. Simulation of a needle electrode

We simulated needle electrodes by a simplified version of the CST described in [48]. In general, the presence of an electrode imposes a fixed electrostatic potential along its surface. However, one can retain the main properties of a needle electrode by fixing the potential only at its tip (point P in figure A1). This is achieved by introducing a simulated point charge Q at a certain location inside the electrode. At each time step of the simulation, the value of Q is calculated to keep $\phi(P)$ (the electrostatic potential at P) fixed to $\phi(P) = V_0$. This schematic approach approximates the effect of a needle with a radius equal to the distance between P and Q (R_{needle}

in figure A1) and a length equal to the distance between the upper planar electrode and Q (L_{needle} in figure A1).

In our simulations, we restrict the particles to the cylindrical volume below the needle tip and apply a homogeneous Neumann boundary condition at its top and bottom sides. Although this creates an artificial boundary inside the physical domain, note that our streamers will touch this plane only around the needle tip. Hence it can be used as a rough approximation for an electrode with a free in- or outflow of electrons.

References

[1] Raizer Yu P 1991 *Gas Discharge Physics* (Berlin: Springer)
[2] Briels T M P, Kos J, Winands G J J, van Veldhuizen E M and Ebert U 2008 *J. Appl. D: Appl. Phys.* **41** 234004 (this issue) (arXiv:0805.1376)
[3] Bazelyan E M and Raizer Yu P 1998 *Spark Discharge* (Boca Raton, FL: CRC Press)
[4] Pasko V P and Stenbaek-Nielsen H-C 2002 *Geophys. Res. Lett.* **29** 82
[5] Williams E R 2006 *Plasma Sources Sci. Technol.* **15** S91
[6] Brau F, Luque A, Meulenbroek B, Ebert U and Schäfer L 2008 *Phys. Rev.* E **77** 026219
[7] Luque A, Brau F and Ebert U 2008 *Phys. Rev.* E **78** 016206 (arXiv:0708.1722)
[8] Winands G J J, Liu Z, Pemen A J M, van Heesch E J M, Yan K and van Veldhuizen E M 2006 *J. Phys. D: Appl. Phys.* **39** 3010
[9] Winands G J J, Liu Z, Pemen A J M, van Heesch E J M and Yan K 2008 *J. Phys. D: Appl. Phys.* **41** 234001 (this issue)
[10] Winands G J J 2007 Efficient streamer plasma generation *PhD Thesis* Eindhoven University of Technology, The Netherlands http://www.tue.nl/bib
[11] van Heesch E J M, Winands G J J and Pemen A J M 2008 *J. Phys. D: Appl. Phys.* **41** 234015 (this issue)
[12] Wang M C and Kunhardt E E 1990 *Phys. Rev.* A **42** 2366
[13] Dhali S K and Williams P F 1987 *J. Appl. Phys.* **62** 4696
[14] Kossyi I A, Kostinsky A Y, Matveyev A A and Silakov V P 1992 *Plasma Sources Sci. Technol.* **1** 207
[15] Babaeva N Y and Naidis G V 1996 *J. Phys. D: Appl. Phys.* **29** 2423
[16] Abdel-Salam M, Nakano M and Mizuno A 2007 *J. Phys. D: Appl. Phys.* **40** 3363
[17] Bourdon A, Pasko V P, Liu N Y, Célestin S, Ségur P and Marode E 2007 *Plasma Sources Sci. Technol.* **16** 656
[18] Luque A, Ebert U, Montijn C and Hundsdorfer W 2007 *Appl. Phys. Lett.* **90** 081501
[19] Pancheshnyi S, Nudnova M and Starikovskii A 2005 *Phys. Rev.* E **71** 016407
[20] Pancheshnyi S 2005 *Plasma Sources Sci. Technol.* **14** 645
[21] Yi W J and Williams P F 2002 *J. Phys. D: Appl. Phys.* **35** 205
[22] Pancheshnyi S V and Starikovskii A Y 2003 *J. Phys. D: Appl. Phys.* **36** 2683
[23] Kulikovsky A A 1994 *J. Phys. D: Appl. Phys.* **27** 2564
[24] Babaeva N Y and Naidis G V 1997 *IEEE Trans. Plasma Sci.* **25** 375
[25] Liu N and Pasko V P 2004 *J. Geophys. Res.* **109** A04301
[26] Pasko V P 2007 *Plasma Sources Sci. Technol.* **16** 13
[27] Luque A *et al* 2008 *Phys. Rev. Lett.* **101** 075005
[28] Montijn C, Hundsdorfer W and Ebert U 2006 *J. Comput. Phys.* **219** 801
[29] Li C, Brok W J M, Ebert U and van der Mullen J J A M 2007 *J. Appl. Phys.* **101** 123305
[30] Montijn C and Ebert U 2006 *J. Phys. D: Appl. Phys.* **39** 2979
[31] Li C, Ebert U and Brok W J M 2008 *IEEE Trans. Plasma Sci.* **36** 910 (arXiv:0712.1942)
[32] Li C, Ebert U, Brok W J M and Hundsdorfer W 2008 *J. Phys. D: Appl. Phys.* **41** 032005
[33] Briels T M P, Kos J, van Veldhuizen E M and Ebert U 2006 *J. Phys. D: Appl. Phys.* **39** 5201
[34] Briels T M P, van Veldhuizen E M and Ebert U 2008 *J. Phys. D: Appl. Phys.* **41** 234008 (this issue)
[35] van Veldhuizen E M, Rutgers W R and Ebert U 2002 Branching of streamer type corona discharge *Proc. 14th Int. Conf. Gas Discharges and their Applications (Liverpool, UK)*
[36] Briels T M P 2007 Exploring streamer variability in experiments *PhD Thesis* Eindhoven University of Technology, The Netherlands
[37] Ebert U, van Saarloos W and Caroli C 1997 *Phys. Rev.* E **55** 1530
[38] Lagarkov A N and Rutkevich I M 1994 *Ionization Waves in Electrical Breakdown in Gases* (New York: Springer)
[39] Pancheshnyi S V and Starikovskii A Y 2001 *J. Phys. D: Appl. Phys.* **34** 248
[40] Kulikovsky A A 2000 *J. Phys. D: Appl. Phys.* **33** 1514
[41] D'yakonov M I and Kachorovskii V Yu 1988 *Sov. Phys.—JETP* **67** 1049
[42] D'yakonov M I and Kachorovskii V Yu 1989 *Sov. Phys.—JETP* **68** 1070
[43] Raizer Yu P and Simakov A N 1998 *Plasma Phys. Rep.* **24** 700
[44] Ebert U, Montijn C, Briels T M P, Hundsdorfer W, Meulenbroek B, Rocco A and van Veldhuizen E M 2006 *Plasma Sources Sci. Technol.* **15** S118
[45] Pancheshnyi S and Starikovskii A Y 2004 *Plasma Sources Sci. Technol.* **13** B1
[46] Montijn C, Ebert U and Hundsdorfer W 2006 *Phys. Rev.* E **73** 065401
[47] Nijdam S, Moerman J S, Briels T M P, van Veldhuizen E M and Ebert U 2008 *Appl. Phys. Lett.* **92** 101502
[48] Singer H, Steinbigler H and Weiss P 1976 *IEEE Trans. Power Appar. Syst.* **93** 1660